TOPOGRAPHY CHANGE AROUND RIVER MOUTH

I. Deguchi, S. Araki and members of Topic-2

Department of Civil Engineering, Osaka Univercity, Yamada-oka 2-1, Suita, Osaka 565-0871, Japan

ABSTRACT

This is an interim report of a goup in Topic-2 of the Core University Program. The final objective is to investigate the mechanism of beach erosion and propose counter measures including software and hardware. In this report, methodology to analyze the topography change that shoud be utilized in the analysis of topography change in some coasts in Vietnam are reviewed. Points at issue we have to solve and the data we need for applying methodology to the coast in Vietnam are discussed.

KEYWORDS

river mouth sand bar, river discharge, waves and wave-induced current, numerical model, beach erosion

INTRODUCTION

Coastline especially sandy beach change its configuration day by day. The amound of daily change is not so large but the accumulation of daily change creates large scale characteristic topography in the coastal region that appears even in the topographical map of the scale 1/50000 for a long time. A large scale topography change also takes place within a short time under the occasional attacks of extreme external force such as rough waves, flooding and so on. In the days when people did not utilize the coastal region, such kind of topography change had noting to do with their social and economic activities.

Coastal region in Vietnam has been developing for various purposes. A lot of mangrove forest that used to function as barriers to external forces in the coastal region has disappeared to form shrimp pond and so on. As a result, the productivity in the coastal region is gradually increasing and at the same time weakness in the coastal region becomes obvious in many places. Sever coastal erosion in the southern part of Red River river mouth and Cangio District near Saigon River are certainly examples of such weakness.

Topography change of the sandy beach is usually caused by the unbalance of local sediment transport rate. If there is not any coastal structures that bring about unbalance of sediment transport, the behavior of discharged sediment from the river strongly affect the topography change around the river mouth. There are many characteristic topography around river mouth. River mouth sand bar, delta and submerged terrace are the representatives. Various kinds external forces such as river flow, waves and wave-induced current, tidal current develop these bottom topography. Through these topography river mouth behave as source of sand supply to the surrounding coast. The authors have been carrying out series of investigation about the river mouth topography and already developed numerical models for predicting formation and disappearance of the river mouth sand bar.

The aims of this study is to analyze the mechanism of severe beach erosion in the southern part of Red River and Cangio District with relation to the discharged sediment from the river mouth by applying our numerical models. First of all, the outline of the numerical model is explained briefly and then discuss how to apply our models to the river mouths in Vietnam.

NUMERICAL MODEL FOR PREDICTING TOPOGRAPHY CHANGE AROUND RIVER MOUTH

There are various kinds of fluid motions around river mouth and complicated interactions between each fluid motion and bottom topography. Main fluid motions are river flow, waves, wave induced-currents and tidal flow. The authors have already developed three numerical models for simulate fluid motion and topography change around the river mouth. That is, 1) depositional pattern of discharged sediment from the river mouth(model-1), 2)formation of river mouth sand bar by waves and wave-induced current(model-2) and 3)flushing of river mouth sand bar by flooding(model-3).

In this section, first of all, fundamental equations that govern fluid motion and sediment transport are shown and then characteristics of three numerical models and their applicability is discussed.

Fundamental Equations

Fluid motion around the river mouth is characterized by the flesh river flow, waves and wave-induced current and tidal current. Therefore, density difference between the flesh water and the sea play very important roll in various phenomena around the river mouth. On the other hand, the authors developed numerical models aiming at special event where there is a strong river discharge(model-1 and -3) or there is not any river discharge(model-2). When there is a strong river discharge, the flow around the river mouth is usually strongly mixed and density difference can be ignored in the vicinity of the river mouth. So the authors use a usual depth and time averaged shallow water equations in the coordinate system shown in Fig.1 to evaluate time averaged flow characteristics. Here, the expression "time averaged" means to take time average over a few wave periods and does not mean a perfect steady state.

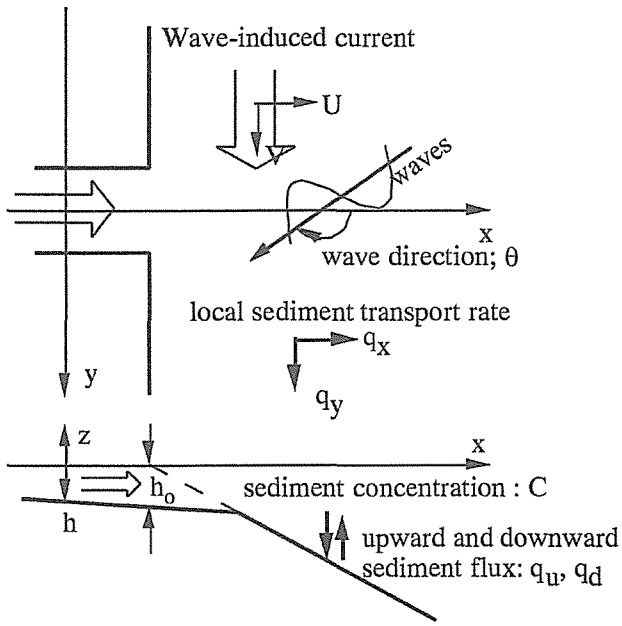

Fig.1 Coordinate system and definition

x-axis is taken in the offshore from the river mouth as defined in the figure and y-axis is in the longshore direction. Incident wave angle θ is measured as defined in the figure. U and V are the wave-induced current velocity in x- and y-directions, h is the water depth and $\overline{\eta}$ is the mean surface displacement. Using these notations, the equation of continuity and ėquation of motion are expressed as follows:

$$\frac{\partial \overline{\eta}}{\partial t}+\frac{\partial}{\partial x}\left\{U(h+\overline{\eta})\right\}+\frac{\partial}{\partial y}\left\{V(h+\overline{\eta})\right\}=0 \tag{1}$$

$$\frac{\partial U}{\partial t}+U\frac{\partial U}{\partial x}+V\frac{\partial U}{\partial y}=-g\frac{\partial \overline{\eta}}{\partial x}-\frac{1}{\rho(h+\overline{\eta})}\left\{\frac{\partial S_{xx}}{\partial x}+\frac{\partial S_{xy}}{\partial y}+\overline{\tau}_{bx}\right\}+R_x \tag{2}$$

$$\frac{\partial V}{\partial t}+U\frac{\partial V}{\partial x}+V\frac{\partial V}{\partial y}=-g\frac{\partial \overline{\eta}}{\partial y}-\frac{1}{\rho(h+\overline{\eta})}\left\{\frac{\partial S_{yx}}{\partial x}+\frac{\partial S_{yy}}{\partial y}+\overline{\tau}_{by}\right\}+R_y \tag{3}$$

where S_{xx}, S_{xy}, S_{yx} and S_{yy} are the radiation stress tensor, $\overline{\tau}_{bx}$ and $\overline{\tau}_{by}$ are the time averaged bottom shear stresses in x and y direction, and R_x and R_y are the lateral mixing terms.

The radiation stress tensors are the functions of wave characteristics,

$$S_{xx} = \frac{\rho g H^2}{8}\left\{\left(2n-\frac{1}{2}\right)\cos^2\theta + \left(n-\frac{1}{2}\right)\sin^2\theta\right\}$$

$$S_{xy} = S_{yx} = \frac{\rho g H^2}{8}\left(\frac{n}{2}\sin 2\theta\right) \tag{4}$$

$$S_{yy} = \frac{\rho g H^2}{8}\left\{\left(2n-\frac{1}{2}\right)\sin^2\theta + \left(n-\frac{1}{2}\right)\cos^2\theta\right\}$$

$$n = \frac{1}{2}\left\{1+\frac{2k(h+\eta)}{\sinh 2k(h+\eta)}\right\}$$

where ρ is the density of water, g is the gravity acceleration, H is the wave height and k is the wave number. For the time averaged bottom shear stress, a conventional expressions derived by Deguchi et al (19) are used

$$\overline{\tau}_{bx} = \frac{1}{2}\rho \cdot f_w \cdot F_c^2 \frac{U}{\sqrt{U^2+V^2}} \text{ and } \overline{\tau}_{by} = \frac{1}{2}\rho \cdot f_w \cdot F_c^2 \frac{V}{\sqrt{U^2+V^2}} \tag{5}$$

where f_w is Jonsson's friction factor and F_c is the function of water particle velocity u_w due to wave motion and wave-induced current velocity.

$$F_c^2 = \frac{1}{2}\hat{u}_w^2 + \frac{1}{4}\left(U^2+V^2\right) \text{ and } \hat{u}_w = \frac{\pi H}{T\sinh kh} \tag{6}$$

For the lateral mixing terms, the following expression with lateral mixing coefficient, k_{xx}, k_{xy}, k_{yx} and k_{yy} derived by Longuett-Higgins are used.

$$R_x = k_{xx}\frac{\partial^2 U}{\partial x^2} + k_{xy}\frac{\partial^2 U}{\partial y^2}, R_y = k_{yx}\frac{\partial^2 V}{\partial x^2} + k_{yy}\frac{\partial^2 V}{\partial y^2} \tag{7}$$

To determine the wave field and radiation stress, a so-called unsteady mild slope equations derived by Nishimura are used.

$$\frac{\partial Q_x'}{\partial t} + c^2\frac{\partial \eta}{\partial x} = 0 \tag{8}$$

$$\frac{\partial Q_y'}{\partial t} + c^2\frac{\partial \eta}{\partial y} = 0 \tag{9}$$

$$\frac{\partial \eta}{\partial t} + \frac{1}{n}\left\{\frac{\partial}{\partial x}\left(nQ_x'\right) + \frac{\partial}{\partial y}\left(nQ_y'\right)\right\} = 0 \tag{10}$$

where Q_x and Q_y are depth integrated mass flux in x- and y-direction and c is the wave celerity.
We can simulate wave transformation including refraction, diffraction, reflection, shoaling and wave decay after breaking. The following wave breaking criteria is used in the model:

$$(Q_x^2 + Q_y^2)^{1/2}/h < 0.3c \tag{11}$$

After wave breaking, the term expressing momentum loss (for example Deguchi, 1998) are added in the right hand side of Eqs,(8) and (9).

Change in the water depth is calculated from the continuity equation of sediment transport.

$$\frac{\partial h}{\partial t} = \frac{1}{1-\lambda}\Delta q \tag{12}$$

where Δq is the spatial gradient of sediment transport rate.

In usual, the non-equilibrium property of sediment transport appears significantly in suspended sediment transport and bed load sediment is insensitive to the non-equilibrium property. Especially, non-equilibrium suspended sediment transport play an important roll around the river mouth. Then Δq is expressed as the sum of the gradient of bed load transport rate and vertical sediment flux at the bottom as follows.

$$\Delta q = \frac{\partial q_{bx}}{\partial x} + \frac{\partial q_{by}}{\partial y} + \Delta q_s \tag{13}$$

To calculate the vertical sediment flux including the effect of non-equilibrium property of suspended sediment, we have to determine nonequilibrium suspended sediment concentration. In our model, we solve the following depeth and time averaged advection-dispersion equation to determine suspended sediment concentration:

$$\frac{\partial \overline{C}}{\partial t} + U\frac{\partial \overline{C}}{\partial x} + V\frac{\partial \overline{C}}{\partial y} = \frac{\partial}{\partial x}\left(K_x\frac{\partial \overline{C}}{\partial x}\right) + \frac{\partial}{\partial y}\left(K_y\frac{\partial \overline{C}}{\partial y}\right) + \frac{1}{h+\overline{\eta}}\left[K_z\frac{\partial c}{\partial z} - w_f c\right]_{z=-h}^{\eta} \tag{14}$$

$$\overline{C} = \frac{1}{h+\eta}\int_{-h}^{\eta} c\,dz$$

The last term of the right hand side of Eq.(14) expresses the vertical flux at the bottom ans is rewritten in the following form for evaluating his term, upward and downward flux:

$$\Delta q_s = \frac{1}{h+\overline{\eta}}\left[K_z\frac{\partial c}{\partial z} - w_f c\right]_{z=-h}^{\eta} = \left[(1-r)\overline{C}_0 w_f\left(1-\frac{u_*}{w_f}\right) + \overline{C}w_f\right] \tag{15}$$

$$u_* > w_f \rightarrow r = 0$$

$$u_* < w_f \rightarrow r = 1$$

where w_f is the settlong velocity of sediment, $\overline{C}_0$ is the reference concentration and $u_* = \sqrt{\overline{\tau}_b/\rho}$ is the shear velocity.

Semi-empirical expression derived by Deguchi et al. (1980) is used to estimate the reference concentration.

$$\overline{C}_0 = 0.347 \cdot N_c^{1.77} \tag{16}$$

$$N_c = \frac{0.688\hat{u}_w^2}{1.13(\rho_s/\rho - 1)\cdot g \cdot w_f \cdot T}$$

where T is the wave period.

K_x and K_y are the dispersion coefficients in x- and y-directions and are evaluated from the Murrary's expression (Murray,1968)

$$K_x = K_y = 0.15 \cdot \bar{U}h \tag{17}$$

The local bed load sediment transport rate is evaluated by using the properly formulated equation (for ex-

amples, Rujin,1985 and Deguchi, 1985). The following is an example (Deguchi et al., 1980) derived based on Sheath formula (Sleath, 1978).

$$q_{bx} = 47\pi\sigma d^2(\psi - \psi_c)^{1.5}(U/\hat{u}_w),\ q_{by} = 47\pi\sigma d^2(\psi - \psi_c)^{1.5}(V/\hat{u}_w) \qquad (18)$$

where $\psi = u_*^2/\sigma' gd$ is the Shields' number and ψ_c is the critical Shields' number for sediment movement.

Depositional pattern of discharged sediment from the river mouth (Deguchi & Sawaragi, 1988)

Numerical model mentioned above was first applied for predicting depositional pattern of discharged sediment from the river mouth that was measured in the model basin. In this case, the transporting agency was river flow. Therefore, the radiation stress term in Eqs.(2) and (3) were omitted and Rijins formula (Rijin, 1985) for bed load transport rate in steady flow was used.

In the numerical simulation, fluid motion was first calculated by solving Eqs.(1)-(3) and then depositional pattern was calculated using Eqs.(13) and (15) together with Rijin's bed load formula. Eqs.(1)-(3) were transformed into a system of difference equations by a so-called ADI method at grid points of isometric mesh of the grid interval Ds=20cm. Transformed difference equations were solved at time interval Dt=0.15s.The boundary condition for river flow was given at the upstream boundary by giving surface elevation.

Figure 2 illustrates the comparison of measured and calculated depositional patterns in the case of fine sand. Discharged velocity at the river mouth was 45cm/s and the mean grain size was 0.15mm. Figure 2(a) is the measured depositional pattern and (b) is the calculated depositional pattern. Figures (c) and (d) are the calculated depositional patterns of bed load and suspended load, respectively.

Calculated change in water depth caused by suspended sediment extends till x=3m but the amount is not so large as that caused by bed load. Bed load material do not expand beyond x=2m that coincides with the critical depth where the bottom shear stress exceeds the critical shear stress of the sediment movement. When compared with Figs.2(a) and (b), the calculated depositional pattern predicts measured pattern fairly well.
Figure 3 shows the comparison of deposited profiles in the cases of fine sand (d=0,15mm, (a)) and coarse sand (d=0.35mm, (b)) along the centerline of the river (y=0). In the latter case, almost all discharged sediment was transported as bed load.

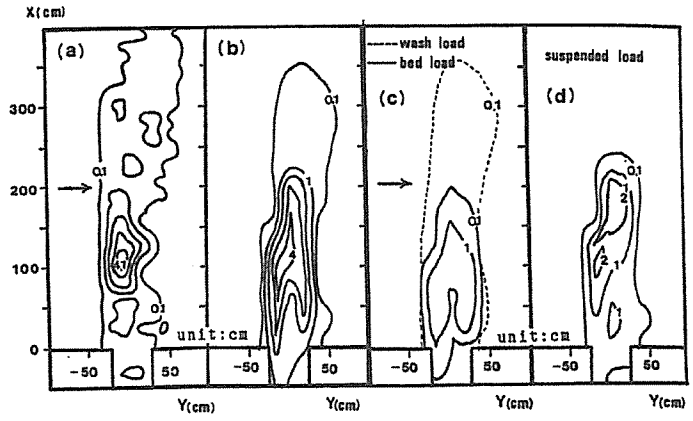

Fig.2 Comparison of measured and calculated depositional pattern of discharged sediment (mean grain size of discharged sediment d=0,15mm, (a):measured depositional pattern, (b):calculated depositional pattern, (c) and (d):cailulated depositional patterns due to suspenden and bed load)

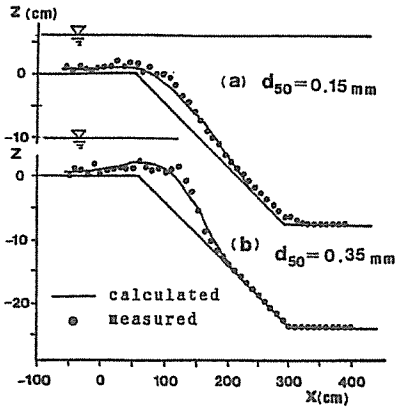

Fig.3 Comparison of measured and calculated profiles of deposited sediment.
((a): d=0.15mm, (b):d=0.35mm)

Formation of river mouth sand bar (Deguchi & Chun, 1997)

The second application is to simulate formation process of river mouth sand bar by waves and wave-induced current. The authors simulated measured formation process of river mouth sand bar in the wave basin. In this case, waves play very important role. Wave field was calculated from Eqs.(8)-(10). These equations were transformed into difference equations at grid points of isotropic mesh of the interval Ds=5cm and were solved transformation at time interval Dt=0.02s. Using the calculated wave field, the radiation stresses were evaluated and wave-induced current was calculated from Eqs.(1)-(3) at the same grid points of wave calculation. Finally the topography change was calculated from Eqs.(13)-(15). Interaction among topography change, wave transformation and resulting wave-induced current were taken into account by iterating above-mentioned calculation at every 10min.

Figures 4 and 5 are examples of the comparison of measured river mouth sand bar (Fig.(a)) and calculated profile of sand bar (Fig.(b)) 60min after the generation of waves. In both cases, The incident wave height H was 6cm and period T was 1.2s. Figure 4 is the case where the initial depth at the river mouth was 6cm and the river mouth was perfectly closed by the sand bar in both calculation and experiment. Figure 5 is the case where the initial depth of the river mouth was 3cm. In this case, the river mouth did not close even 60min after generation of waves in both experiment and simulation. The length of the bar measured in the experiment was about 60cm and almost the same bar was generated at the same place in the simulation.

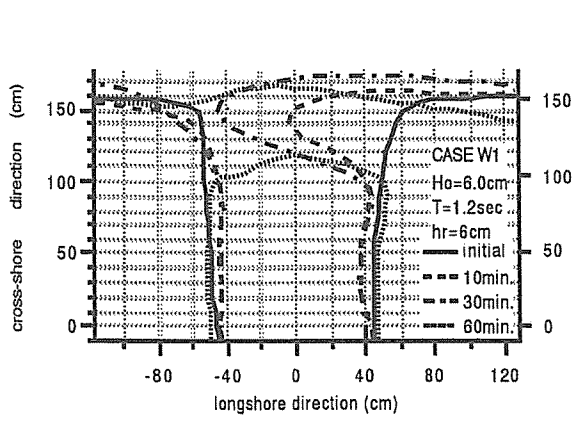

(a) Measured profile of sand bar

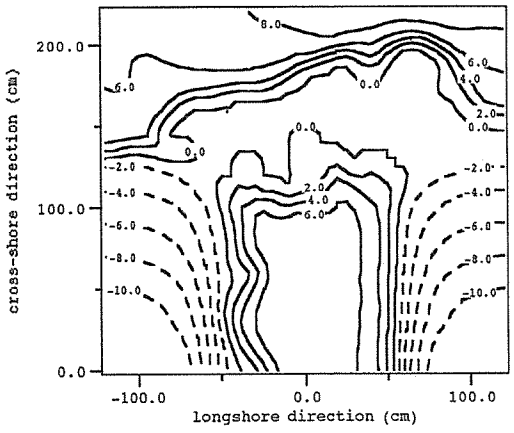

(b) Calculated profile of sand bar

Fig.4 Comparison between measured and calculated profile of sand bar
(Initial depth at the river mouth hr=6cm)

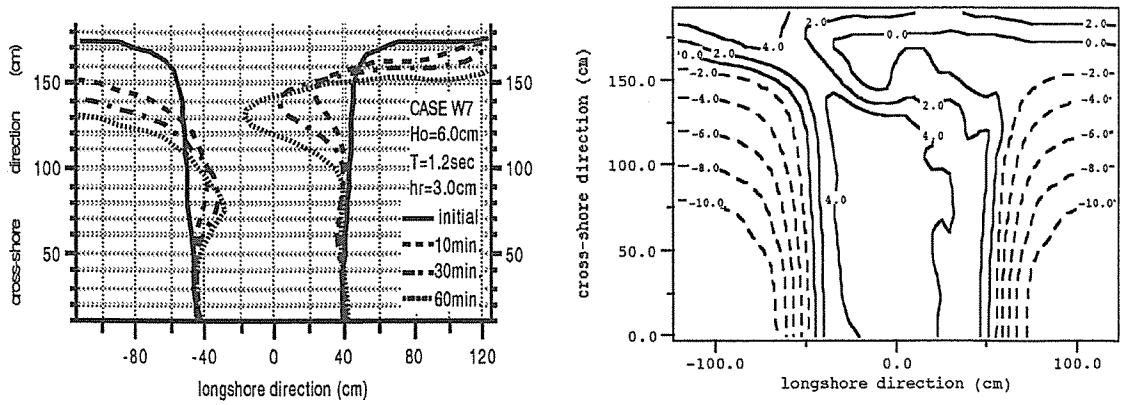

(a) Measured profile of sand bar (b) Calculated profile ofsand bar

Fig.5 Comparison between measured and calculated profile of sand bar
(Initial depth at the river mouth hr=3cm)

Flushing of river mouth sand bar by flood (Deguchi & Chun, 2000)

The last application is to simulate measured flushing process of river mouth sand bar in the experiment. In this case, the unique external force was the flood. Therefore, the radiation stresses in Eqs(2) and (3) were ignored. The same numerical procedure was applied as the case of the simulation of depositional pattern of discharged sediment. The boundary condition for flood was given by water level and velocity measured in the river at the upstream side of the calculation region in the experiment. A so-called moving boundary condition was applied to determine the shoreline. Flow field was first calculated at the grid points set at the distance of Ds=5cm at time interval Dt=0.02s. Then the topographic change was calculated to determine bottom topography for calculating next step of flow. These calculations were iterated at time interval of one second to take into account of the interaction between topography change and flow. Figures 6 and 7 shows two examples of comparisons between calculated topography change caused by the same model flood and the measured results to examine the applicability of the numerical model. The model flood continued for 31min.

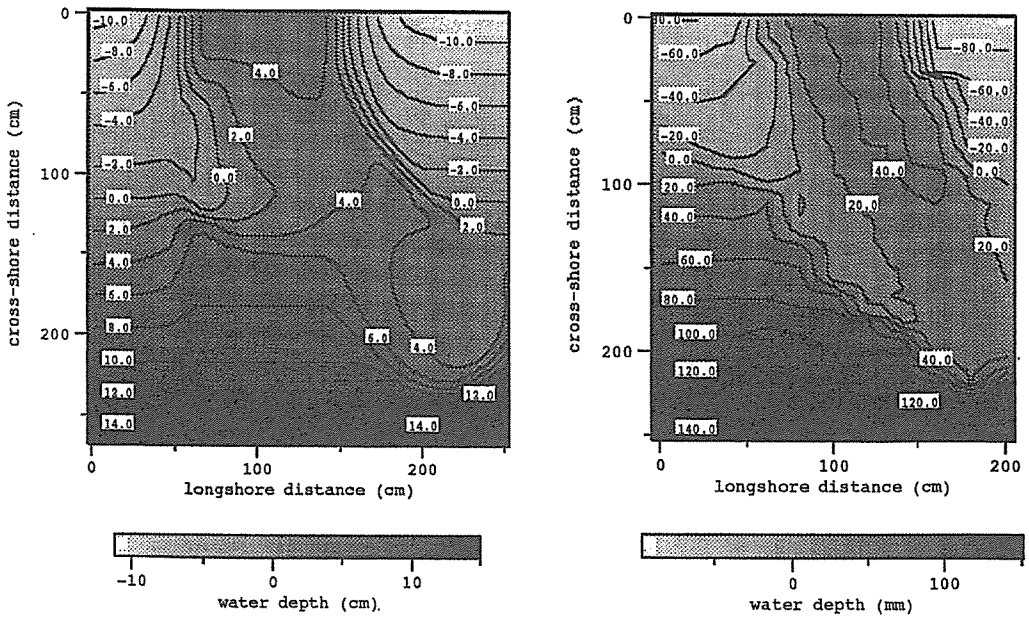

(a) Calculated topography cange (b)Measered topography cange

Fig.6 Comparison of measured and calculated topography cange in tee case of low bar

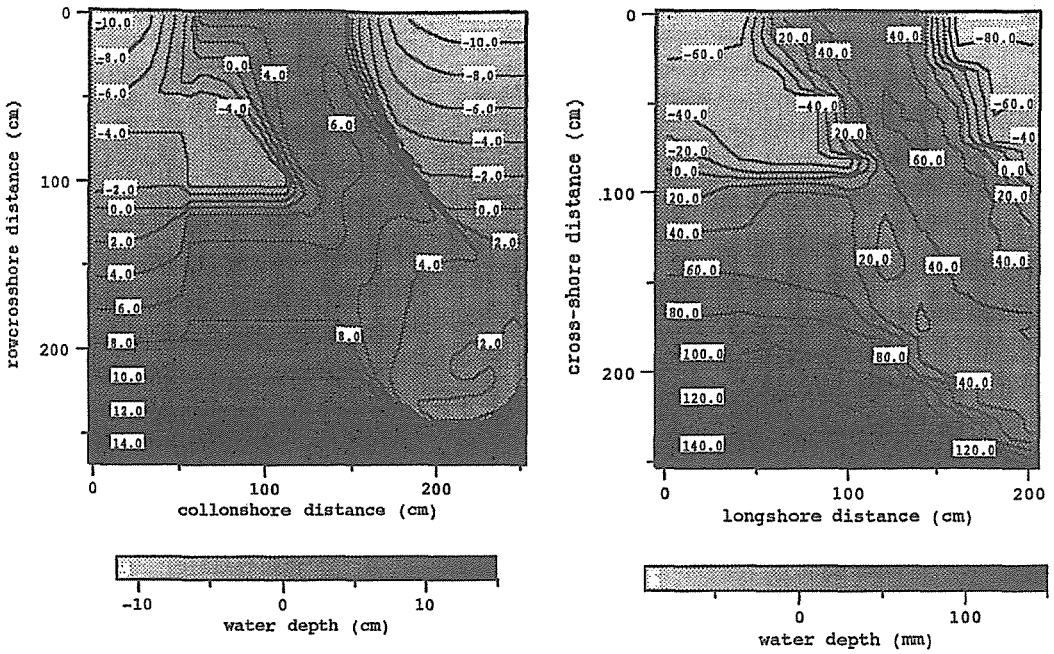

(a) Calculated topography cange (b)Measered topography cange

Fig.6 Comparison of measured and calculated topography cange in tee case of high bar

In the case shown in Fig.6, the height of initial sand bar was 3cm and the bulk flushing of river mouth bar together with the both side bank erosion took place in the experiments. Calculated profile reproduces the measured profile well. The initial height of the bar shown in Fig.7 was 6cm. In this case, only side bank erosion took place and part of sand bar disappeared in the experiment. Again, the measured deformation is well reproduced by the numerical model.

APPLICATION OF NUMERICAL MODEL TO SOME RIVER MOUTH IN VIETNAM

There are large rivers in two objective coast in Vietnam where sever beach erosion is taking place. That is, Red River in northern part and Saigon River in southern part. Discharged sediment from these rivers seems to have something to do with erosion. The member of Topic 2 started the project to investigate the mechanism with relation to the behavior of river mouth topography and discharged sediment from the river mouth.

In the investigation, numerical model will surely be a powerful tool. So, the authors try to apply the above mentioned numerical model for simulating behavior of river mouth topography. Among various factors that affects the river mouth topography, the effects of river flow and waves are estimated by the numerical model. Although the effect of the tidal current is also evaluated by the numerical model formally, the validity of the numerical model at this point is not confirmed yet. Because of the relatively large tidal range along the coastline in Vietnam we have to establish the procedure to cope with the large tidal range.

Any way, the quantities we have to know before the numerical simulation are as follows:

- Detailed bottom topography of the calculation region including flood plane
- Measured typical topography change to know the characteristics of sediment movement and calibrate nu merical model
- Representative hydrograph (relation between water level and flow rate) of river discharge
- Relation between flow rate and concentration of wash load to determine boundary condition at the upstream side of the calculation region
- Grain size in the objective river to determine concentration of bed material load

- Garin size distribution in the objective coastal region to know predonimant direction of sediment transport due to waves
- Wave climate throuth the whole year in the objective regions
- Tidal range and flow pattern of tidal current in the objective region

The authors are currently collecting these data. Among them, we are now analyzing satelite image(JERS) to investigate characteristics of topography change.

CONCLUSIONS

Tne numerical model that we are going to apply to some coasts in Vietnam are reviewed and data we require for the simulation are disucussed. We are now calbrating our numerical model to fix some empirical coefficients in our model.

References

Deguchi, I. and T. Sawaragi (1988), Effects of Structure on Deposition of Discharged Sediment around River mouth, Proc. 21st ICCE, ASCE, pp.1573-1587.

Deguchi, I. and S. K. Chun (1997), Formation of river-mouth sand bar by waves and wave-induced current, Proc. 7th ISOPE, pp.877-884.

Murray, S. P., (1968), Simulation of horizontal turbulent diffusion of particle under waves, Proc. 10th ICCE, ASCE, pp.446-466.

Rijin, L. C., (1985), Sediment transport, Delft Hydraulic Labo., Publ. No. 334.

Sleath, J. F. A. (1978), Measurement of bed load in oscillatory flow, J., WPCO Div., Proc. ASCE, Vol. 104, No. ww4, pp.291-307.